

Skyrmion stars and the multilayered rational map ansatz

Susan Nelmes* and Bernard M. A. G. Piette†

Department of Mathematical Sciences, University of Durham, Science Laboratories, South Road, Durham. DH1 3LE. United Kingdom

(Received 25 July 2011; published 18 October 2011)

We investigate the large baryon number sector of the Einstein-Skyrme model as a possible model for baryon stars and construct low energy configurations that resemble neutron stars. Previous studies have shown that gravitating Skyrmions produced by using rational maps can achieve spherically symmetric, multibaryon-bound states at large baryon numbers, but these configurations were hollow shells. In this paper, we improve on the previous work by constructing configurations corresponding to solid spheres with a radius-dependent baryon density.

DOI: [10.1103/PhysRevD.84.085017](https://doi.org/10.1103/PhysRevD.84.085017)

PACS numbers: 12.39.Dc, 04.40.-b, 26.60.-c, 97.60.Jd

I. INTRODUCTION

The Skyrme model is a nonlinear theory of pions originally proposed by T. H. R. Skyrme in 1961 [1,2], that has topological soliton solutions, known as Skyrmions, which are identified as baryons. The Skyrmions possess a conserved topological charge which is interpreted as the baryon number. The model was set aside after the discovery of QCD in the late 1960s but was later [3] shown to be an approximate, low energy, effective field theory for QCD which becomes more exact as the number of quark colors becomes large, and has been successful in modeling the structures of various nuclei.

The Einstein-Skyrme model couples the Skyrme model to gravity and has been previously studied in [4–6]. The coupling of the Skyrme model to gravity is particularly interesting when considering astrophysical objects, with black hole formation having been studied in [7,8].

This paper continues the work of [9] which studied large baryon number Skyrmions in the Einstein-Skyrme model and configurations of such Skyrmions in an attempt to investigate if stable solitonic stars could exist within the model. The first study into this topic [4] predicted that such stars would be unstable, however, this work used the hedgehog ansatz which is unstable for baryon number greater than one even before the Skyrme model is coupled to gravity.

The discovery [10,11] that stable shell-like solutions to the Skyrme model can be produced using the rational map ansatz led to the work in [9]. It was found, after an approximation to allow the solution to be found numerically, that for a baryon number comparable to that of a neutron star (of order 10^{57}) a shell-like stable solution could be found. Further to this, by stacking a number of these shell-like solutions together to form a hollow sphere, a model of a neutron star could be found with an acceptable radius. However, this model still has unrealistic features,

such as a hollow center and an artificially constructed density profile, which this paper improves upon.

In this paper, we first outline the Einstein-Skyrme model, including the first results found by Bizon and Chmaj [4] using the hedgehog ansatz. The previous work by Piette and Probert [9] is then reviewed, introducing the rational map ansatz and studying the results, before considering an improved ansatz to this model, the multilayer ansatz. This is introduced and the results of implementing it are studied. In contrast to the previous work which had produced hollow solutions, we construct configurations that are solid spheres with a radius-dependent baryon density.

II. THE EINSTEIN-SKYRME MODEL

The Einstein-Skyrme model is described by the action

$$S = \int_{\mathcal{M}} \sqrt{-g} \left(\mathcal{L}_{Sk} - \frac{R}{16\pi G} \right) d^4x, \quad (1)$$

which combines the action of the standard Skyrme model for the matter field and the Einstein-Hilbert action for the gravitational field, all defined on the manifold \mathcal{M} . The Lagrangian density for the Skyrme model, \mathcal{L}_{Sk} , is defined as

$$\begin{aligned} \mathcal{L}_{Sk} = & \frac{F_\pi^2}{16} \text{Tr}(\nabla_\mu U \nabla^\mu U^{-1}) \\ & + \frac{1}{32e^2} \text{Tr}[(\nabla_\mu U)U^{-1}, (\nabla_\nu U)U^{-1}]^2 \\ & + \frac{F_\pi^2 m_\pi^2}{8} (\text{Tr}(U) - 1), \end{aligned} \quad (2)$$

where U is an $SU(2)$ matrix and F_π , e and m_π are the pion decay constant, the Skyrme coupling, and the pion mass term, respectively. The Skyrme field is a map from \mathbb{R}^3 to S^3 , the group manifold of $SU(2)$, but finite energy considerations imply that the field at spatial infinity should map to the same point, meaning the Skyrme field is a map between two three-spheres. Such maps fall into homotopy classes indexed by an integer, known as the topological charge, which is interpreted as the baryon number.

*s.g.nelmes@durham.ac.uk

†b.m.a.g.piette@durham.ac.uk

The choice of metric is determined by the fact that large baryon stars are being studied. While most of the Skyrme configurations studied do not possess exact spherical symmetry, as the baryon number increases to that of a realistic neutron star, the spherical symmetry of the solutions becomes more enhanced, to the effect that the discrepancy between the symmetries will not be significant. Also, at high baryon numbers, it can be shown that the gravitational backreaction is small compared to the Skyrme interaction. The spherically symmetric metric used is that associated with the line element

$$ds^2 = -A^2(r)\left(1 - \frac{2m(r)}{r}\right)dt^2 + \left(1 - \frac{2m(r)}{r}\right)^{-1} dr^2 + r^2(d\theta^2 + \sin^2\theta d\phi^2). \quad (3)$$

Here, $A(r)$ and $m(r)$ are radial profile functions which must be determined when solving the model.

From the metric (3), the Ricci scalar can be calculated as

$$R = \frac{-2}{Ar^2}(-A''r^2 - 2A'r + 2A''rm + A'm + 3A'rm' + Arm'' + 2Am'). \quad (4)$$

We must also add a boundary term,

$$S_{\text{GH}} = \frac{-1}{2G} \int m(\infty) dt, \quad (5)$$

to the gravitational term in the action to include the necessary contribution from the boundary of the manifold. This ensures that when the action is varied with respect to the metric, and this variation is set to zero, Einstein's equations are implied [12]. The gravitational action can then be simplified to

$$S_{gr} = \int A(r) \left(\frac{-m'(r)}{G} \right) dr + \frac{m(\infty)}{G}. \quad (6)$$

It is convenient to combine the parameters of the model into one dimensionless coupling constant, α . This can be done by scaling to dimensionless variables, $x = eF_\pi r/2$, $\mu = eF_\pi m/2$, and $\mu_\pi = 2m_\pi/(eF_\pi)$, resulting in $\alpha = \pi G F_\pi^2/2$. For the realistic values of $F_\pi = 186$ Mev and the gravitational constant, G , $\alpha = 7.3 \times 10^{-40}$.

In the first study of gravitating Skyrmions by Bizon and Chmaj [4] (with the pion mass, μ_π , set to zero), the hedgehog ansatz for the Skyrme field was taken

$$U = \exp[i\vec{\sigma} \cdot \hat{r} F(r)], \quad (7)$$

with boundary conditions, $F(x=0) = \mathcal{B}\pi$ and $F(x=\infty) = 0$, where \mathcal{B} is the Baryon number associated with the Skyrme configuration.

They found two branches of global solitonic solutions at each baryon number which annihilate at a critical value of the coupling parameter, α_{crit} , which decreases with increasing baryon number. However, using this ansatz the

solutions for baryon number greater than one are found to be unstable, as they are in the nongravitating case.

III. THE RATIONAL MAP ANSATZ

Introduced by Houghton *et al.* [11,13], the rational map ansatz produces approximate solutions to the Skyrme model. These solutions are not in general radially symmetric but the ansatz decomposes the field into a radial profile function and a rational map.

The ansatz is defined using polar coordinates in \mathbb{R}^3 and setting the stereographic coordinates $z = \tan(\theta/2)e^{i\phi}$. The Skyrme field is then defined as [11]

$$U = \exp(i\vec{\sigma} \cdot \hat{n}_{\mathcal{R}} F(x, t)), \quad (8)$$

where

$$\hat{n}_{\mathcal{R}} = \frac{1}{1 + |\mathcal{R}|^2} (2\Re(\mathcal{R}), 2\Im(\mathcal{R}), 1 - |\mathcal{R}|^2), \quad (9)$$

is a unit vector and \mathcal{R} a rational function of z .

The boundary conditions are set to

$$F(x=0) = \pi, \quad F(x=\infty) = 0. \quad (10)$$

Using this ansatz, the degree of the rational map is equal to the baryon number.

Substituting this rational map ansatz (8) into the action for the model and scaling to dimensionless variables as earlier, we obtain the following reduced Hamiltonian

$$H = \frac{2}{eF_\pi G} \left[\int_0^\infty \left[-A(x)\mu'(x) + A(x)\alpha \times \left[S(x)F(x)^2 x^2 + 2\mathcal{B}\sin^2 F(x)(1 + S(x)F(x)^2) + \frac{I\sin^4 F(x)}{x^2} + \mu_\pi^2 x^2 (2 - \cos g) \right] \right] dx + \mu(\infty) \right], \quad (11)$$

where

$$S(x) = 1 - \frac{2\mu(x)}{x}, \quad (12)$$

and I depends on the chosen rational map. For low baryon number configurations, the rational map that minimises I must be chosen, as has been done in [11,14], but for large baryon numbers the approximation $I \approx 1.28\mathcal{B}^2$ can be used [14].

From this Hamiltonian, the field equations for $F(x)$, $A(x)$ and $\mu(x)$ can be obtained. The previous study [9] of stable solitonic stars attempted to solve these field equations (with the pion mass, μ_π , set to zero) to produce solutions that would model realistic neutron stars.

The profile functions of the solutions found provided motivation for the next approximation. The radial profile function $F(x)$ stays approximately at its boundary value, π , for a finite radial distance before decreasing monotonically over some small region and finally attaining its second boundary value, 0. A similar behavior is seen for both the

mass field, $\mu(x)$, and the metric field, $A(x)$ [9]. As the baryon number is increased, the shell-like structure becomes more pronounced, with the distance before the fields change (shell radius) increasing significantly, while the distance over which the fields change (shell width) settles to a constant size.

In [9], it was considered if these shell-like gravitating Skyrmions could be stacked as more than one layer. This was achieved by modifying the boundary conditions to

$$F(x=0) = N\pi, \quad (13)$$

$$F(x=\infty) = 0, \quad (14)$$

where N is the number of shells, an idea first used for the pure Skyrme model in [13]. The baryon number is now N times the degree of the rational map and this configuration results in energetically favorable solutions when compared to single-layer solutions of the same baryon number. The limitation on this method, however, is that the resulting stacked shells all have the same baryon number and also the same width. Realistically, it is expected that the baryon number should vary significantly over the shells, as well as their width.

To study the high baryon numbers of interest when modeling an object such as a neutron star (of order 10^{57}), a further approximation was introduced in [9] due to the field equations becoming increasingly difficult to handle numerically. This ramp profile approximation replaces the profile functions by those which are piecewise linear, an idea first used in [15,16]. It was shown that this approximation is in good agreement with the rational map ansatz solutions, and by using it, solutions with a very high number of baryons existing as N thin shells of small thickness stacked together can be produced numerically. The solutions at these high baryon numbers are still found to be stable and, at the critical number of layers before there ceases to be any solutions, the radius of the star is approximately 20.91 km, comparable to a neutron star with a typical radius of 10 km.

IV. THE MULTILAYER ANSATZ

While keeping the stacked shell structure of the rational map ansatz model, we wish to improve it by allowing the number of baryons in each shell, b_i , and the widths of the shell, W_i , to vary. The radial charge density is given by $B_i = b_i/W_i = -F(x)'b_i/\pi$, where $F(x)$ is again the radial profile function. This is due to the approximation, $-F(x)' \approx \pi/W_i$, which arises from the fact that the radial profile function varies between $n\pi$ and $(n-1)\pi$ for an integer n over one layer of width W_i . We replace the topological charge (baryon number) of each shell b_i by a shell charge field, $b(x)$, resulting in the total baryon number

$$\mathcal{B} = - \int_0^R b(x) \frac{F(x)'}{\pi} dx, \quad (15)$$

where R is the total radius of the star which can be varied. The approximation, also used in [9], $\int G(x)\sin^p F(x)dx \approx \int G(x_0)\sin^p F(x)dx$ for any function $G(x)$ that varies very little over the width of the shell and the fact that

$$\int_{x_0-W_i/2}^{x_0+W_i/2} \sin^p F(x)dx = \frac{W_i}{\pi} \int_0^\pi \sin^p y dy, \quad (16)$$

allows the Hamiltonian (11) to be reduced to

$$H = \frac{2}{eF_\pi G} \left[\int_0^R \left[-A(x)\mu'(x) + A(x)\alpha \right. \right. \\ \times \left[S(x)F(x)^2 x^2 + b(x)(1 + S(x)F(x)^2) \right. \\ \left. \left. + 1.28b(x)^2 \frac{3}{8x^2} + 2\mu_\pi^2 x^2 \right] dx + \mu(\infty) \right]. \quad (17)$$

Here, the large baryon number approximation $I \approx 1.28b(r)^2$ [14] has been used and $S(x) = 1 - \frac{2\mu(x)}{x}$. The boundary conditions are

$$F(x=0) = N\pi, \quad (18)$$

$$F(x=R) = 0, \quad (19)$$

where N is the number of shells and the radius $R = \sum_{i=1}^N W_i$. The average width of the shells, W , is defined as $W = R/N$.

After defining $q(x) = b(x)/x^2$ for convenience and re-scaling using $F(x) = f(x)N$, $x = Ny$, and $\mu(x) = N\nu(x)$, the Hamiltonian can be rewritten as

$$H = \frac{2N^3}{eF_\pi G} \int_0^W \left[-A(y) \frac{\nu'(y)}{N^2} + A(y)\alpha y^2 \right. \\ \times \left[\left(1 - \frac{2\nu(y)}{y} \right) f(y)^2 (1 + q(y)) + q(y) \right. \\ \left. \left. + 1.28q(y)^2 \frac{3}{8} + 2\mu_\pi^2 \right] dy + \frac{2N\nu(\infty)}{eF_\pi G}, \quad (20)$$

and the total baryon number as

$$\mathcal{B} = -N^3 \int_0^W q(y) \frac{f(y)'}{\pi} y^2 dy. \quad (21)$$

The Hamiltonian (20) is then minimized over $f(y)$, $\nu(y)$, $A(y)$, $q(y)$, W , and N for a given baryon number. This has been done by using simulated annealing over 250 points with 10^8 iterations to find the minimum form of the $f(y)$ and $q(y)$ fields while using the Euler-Lagrange equations to calculate the $\nu(y)$ and $A(y)$ fields using a fourth-order Runge-Kutta method, obtaining the respective profile functions for a given W and N . The minimum energy solution over varying W and N can then be found. Table I presents the results of this minimization for various baryon numbers, all for a zero pion mass.

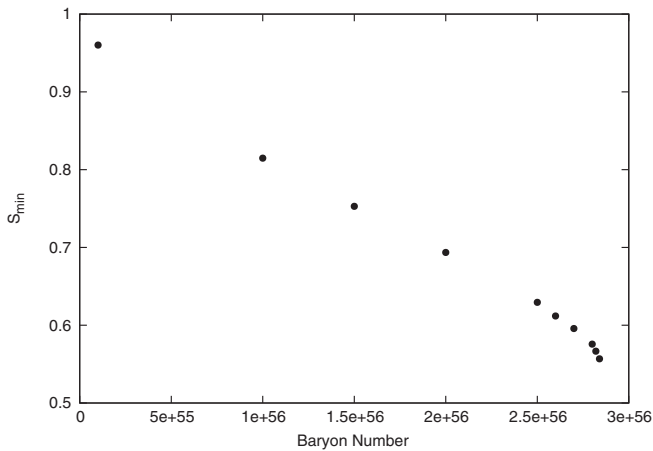
We find solutions up to a baryon number of $\mathcal{B} = 2.84 \times 10^{56}$. For $\mathcal{B} = 2.85 \times 10^{56}$ and above, no minimum

TABLE I. Table of properties of the minimum energy solutions of the Hamiltonian (20).

\mathcal{B}	N	$W(fm)$	Energy/ $\mathcal{B}(\frac{2}{eF_{\pi G}})$	$R(m)$	S_{\min}
1.0×10^{10}	1.250×10^3	1.40	7.76487×10^{-39}	1.75439×10^{-12}	1×10^6
1.0×10^{20}	2.700×10^6	1.40	7.76481×10^{-39}	3.78947×10^{-9}	1×10^6
1.0×10^{30}	5.850×10^9	1.40	7.76479×10^{-39}	8.21053×10^{-6}	1×10^6
1.0×10^{40}	1.250×10^{13}	1.40	7.76489×10^{-39}	1.75439×10^{-2}	1×10^6
1.0×10^{50}	2.700×10^{16}	1.40	7.76474×10^{-39}	37.8947	0.999 982
1.0×10^{55}	1.250×10^{18}	1.40	7.67390×10^{-39}	1754.39	0.960 143
1.0×10^{56}	2.825×10^{18}	1.23	7.32413×10^{-39}	3469.30	0.814 808
1.5×10^{56}	3.350×10^{18}	1.14	7.17409×10^{-39}	3820.18	0.752 900
2.0×10^{56}	3.825×10^{18}	1.05	7.03135×10^{-39}	4026.32	0.693 622
2.5×10^{56}	4.225×10^{18}	0.96	6.88810×10^{-39}	4076.75	0.629 472
2.6×10^{56}	4.375×10^{18}	0.92	6.85854×10^{-39}	4029.61	0.611 816
2.7×10^{56}	4.450×10^{18}	0.90	6.82815×10^{-39}	4001.10	0.595 811
2.8×10^{56}	4.600×10^{18}	0.86	6.79659×10^{-39}	3934.21	0.575 686
2.82×10^{56}	4.650×10^{18}	0.83	6.79004×10^{-39}	3875.00	0.566 545
2.84×10^{56}	4.700×10^{18}	0.81	6.78331×10^{-39}	3813.60	0.556 880

energy solutions for the Hamiltonian, over varying the average width and the number of layers, could be found. This is compared with a baryon number of order 10^{57} for a realistic neutron star. Table I shows that, while the minimum of the function $S(x) = 1 - \frac{2\mu(x)}{x}$ for the minimum energy solution decreases as the baryon number increases, it remains nonzero, meaning that the star has still not collapsed to form a black hole.

Because of the limited accuracy of the numerical methods involved and the fact that solutions with a small S_{\min} may not be easily found, an increase in the number of significant figures for the maximum baryon number for which there are solutions could not be reached. Figure 1 shows how the value of S_{\min} changes with varying baryon number and it can be seen that S_{\min} begins to drop rapidly as the maximum baryon number is reached. It is expected that it will continue to decrease at an increasing pace and any significant increase to the maximum baryon number found will result in a solution that collapses into a black hole. Extrapolating the plot suggests that black hole

FIG. 1. Plot of the value of S_{\min} for various baryon numbers.

collapse occurs at a baryon number of approximately $\mathcal{B} < 3 \times 10^{56}$.

The data shown in Fig. 1, though quite smooth, are affected by various types of numerical errors. First of all, the energy fluctuations during the simulated annealing that have not fully settled within the number of iterations used and around the minimum energy values induce an error that we found to be less than 0.1%. There is also an error due to the sampling nature of the parameter values from which the minimum energy solution has been determined. From interpolating the curve around the minimum energy value, we again find that this error is less than 0.1%. There are also systematic errors due to the discretization of the problem on a lattice that are harder to estimate but we do not expect them to affect the critical value of the baryon number significantly.

Table I shows that as the baryon number is increased the solutions become more and more energetically favorable. This indicates that the solutions are stable and our model can therefore not be ruled out as a model of neutron stars.

At the smaller baryon numbers, the radius grows as $\mathcal{B}^{1/3}$, indicating that the average density of the stars remains constant. The widths of the shells in this region are also seen to remain at a value of 1.40 fm (3.20 in the dimensionless units). Kopeliovich [15,16], calculated the minimum energy value for the width of a shell of a substantial number of baryons in flat space to be $W = \pi$ in the dimensionless units, and as the gravitational interactions are not significant at these smaller baryon numbers, we find there is little deviation from this value here. As the maximum baryon number is approached, the average density of the Skyrmions increases, reaching up to 25 times the density found at the smaller baryon numbers. This indicates that the gravitational interaction becomes more important as the higher baryon numbers are reached.

The increase in density at the higher baryon number recreates the feature found previously in [9] that as the

baryon number approaches its maximum at which a solution can be found, the radius of the star starts to decrease as more baryons are added due to the increasing dominance of the gravitational interactions. This in an interesting property as for realistic neutron stars, the radius must decrease for an increase in mass in order to achieve sufficient degenerate neutron pressure to balance the increased gravitational force.

It is important to note that the baryon density increase for the larger baryon numbers is not just accounted for by the decrease in the widths of the shells found to occur in this region. We find the Skyrmions are compressed in all three directions.

We also note that when compared with realistic neutron stars with a radii of order 10 km, our solutions have radii of appropriate values.

This model only finds solutions up to a baryon number of $\mathcal{B} = 2.84 \times 10^{56}$, and when compared with a realistic neutron star with a baryon number approximately 2×10^{57} , our solutions have 7 times too few baryons. This could be due to the fact that we overestimate the energies of the solutions. For example, the rational map ansatz itself overestimates the energies of the pure Skyrme model by 3% to 4% [11], and using a multiple-shell ansatz has been shown to produce solutions with larger energies than can be found when the solutions are numerically relaxed [13]. This overestimation will cause the solutions to collapse into black holes at a baryon number less than would be realistic.

We now consider the structures of the solutions that have been found, in particular, Fig. 2 shows the radial profile functions for the $f(y)$, $\nu(y)$ and $A(y)$ fields for the maximum baryon number, $\mathcal{B} = 2.84 \times 10^{56}$, for which a solution could be found. We, however, find the same qualitative behavior appearing for all the minimum energy solutions. We recall that the width of the shells is given by $W_i \approx -\pi/f_y$ and it is observed that, as should be

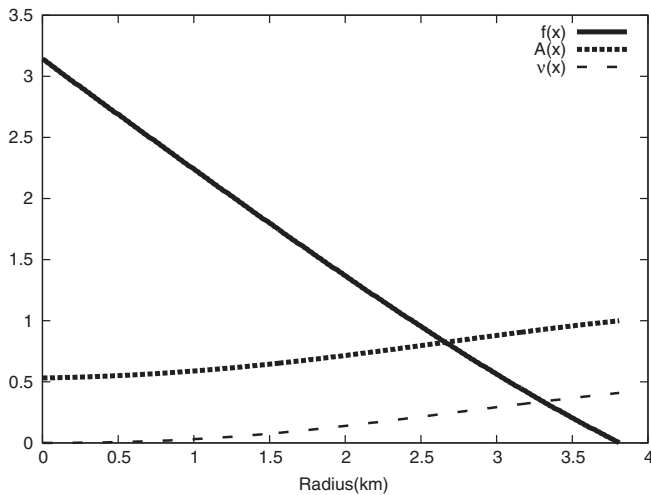


FIG. 2. Plot of the radial profile functions for the dimensionless $f(y)$, $\nu(y)$, and $A(y)$ fields for $\mathcal{B} = 2.84 \times 10^{56}$.

expected, the widths increase as the radius increases, due to less compression for the outer shells from the gravitational interactions.

As the Skyrmions are compressed in the radial direction, they are also compressed laterally, again, with more compression towards the center of the star than towards the edge. Figure 3 shows, by comparing the width of the shells in the radial direction with their size (length) laterally, that this lateral compression becomes more pronounced, when compared with the radial compression, as the center of the star is reached, becoming the dominant reason for the decrease in baryon volume. While the compression would be expected to occur in all directions equally, the structure of the Skyrmions when using the multilayer ansatz may be causing them to shrink more laterally than radially in the high density center of the star.

Because of this radial and lateral compression of the Skyrmions, there is a change in baryon density over the radius of the star. Figure 4 shows that, as expected, the baryon density is high in the center of the star, decreasing as the radius increases.

The observed substantial change in both baryon number per shell, which, for example, ranges from 1.4×10^{36} to 1.1×10^{38} for a total baryon number of $\mathcal{B} = 2.84 \times 10^{56}$, and the widths over the shells, ranging from 0.67–1.00 fm for the same baryon number, justify our improvement to the previous model that allows this to occur.

Solutions found when the pion mass is nonzero can also be considered. In particular, we set $\mu_\pi = 0.2$. The maximum baryon number for which solutions are found decreases to $\mathcal{B} = 2.72 \times 10^{56}$, where again the minimum of the function $S(x) = 1 - \frac{2\mu(x)}{x}$ is still nonzero at 0.551 541. For a given baryon number, the inclusion of the pion mass decreases the average width and the minimum of $S(x)$ while increasing the energy per baryon. The qualitative features of the radial profile functions for the $f(y)$, $\nu(y)$, and $A(y)$ fields are found to be comparable to the zero pion mass case.

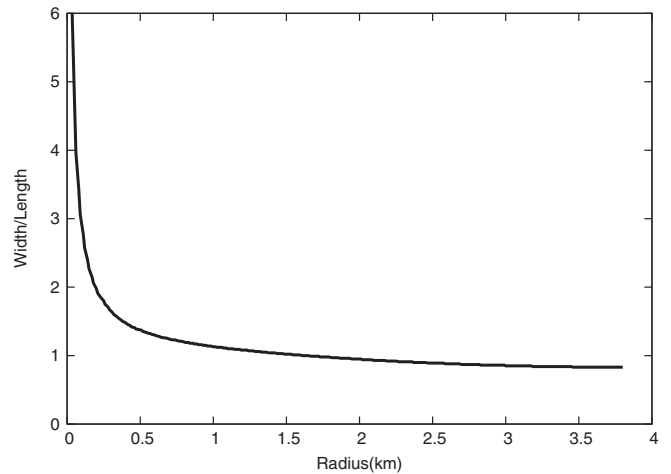


FIG. 3. Plot of the ratio of the width to the length (square root of the cross-sectional area) of the Skyrmions for $\mathcal{B} = 2.84 \times 10^{56}$.

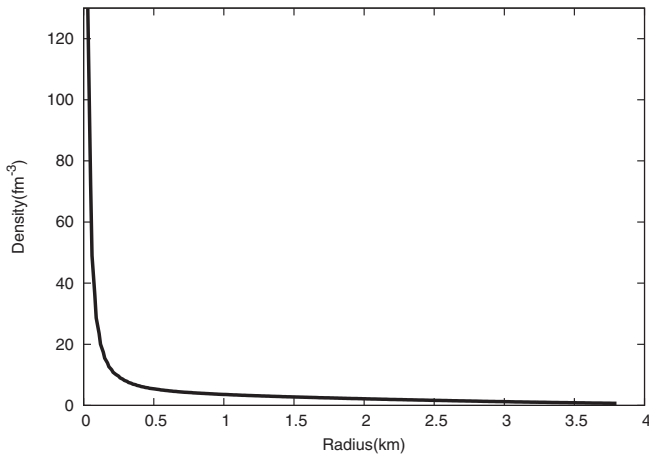


FIG. 4. Plot of the baryon density for $\mathcal{B} = 2.84 \times 10^{56}$.

We note that for baryon numbers between $\mathcal{B} = 5 \times 10^{56}$ and $\mathcal{B} = 2.5 \times 10^{57}$ another minimum energy solution to the Hamiltonian (20) can be found. This solution takes the form of a hollow shell-like structure with a center devoid of baryons, the majority of the baryons located in a dense layer between a narrow range of radii and then another gas-like layer almost completely devoid of baryons. It is expected that these solutions are an artifact of our model and for various reasons, including the unrealistic large hollow center, do not produce suitable models of neutron stars.

V. CONCLUSIONS

Previous work on using the Einstein-Skyrme model to describe stable solitonic stars made use of the rational map ansatz and by doing this, hollow shell-like objects were produced. By stacking these shells together, a more realistic model of a neutron star was produced with an appropriate radius. However, the stacking of the shells was only done naively as the baryon number for all the shells, as well as their width, was kept constant. While for a large baryon number

with few shells this is a reasonable approximation, when many shells are used (such as when modeling an object as large as a neutron star) we would expect a large variation in baryon number across the shells as well as a decrease in the width of the shells towards the center of the star.

In this paper, we have allowed the baryon number to vary across the shells, and also the width of those shells to vary to produce a more realistic description of a neutron star. Stable solutions can be found with radii that compare well with realistic neutron stars which are approximately 10 km in radius, however, solutions could only be found up to $\mathcal{B} = 2.84 \times 10^{56}$ (with a radius of 3813.60 m) while the expectation is that neutron stars should have a slightly larger baryon number of approximately 2×10^{57} . This is likely due to an overestimation of the energy of the solutions produced by the model.

It is interesting to see that as the maximum baryon number for which there is a solution is approached, the radius decreases as more baryons are added, reflecting how real neutron stars behave.

Including a nonzero pion mass into the Skyrme Lagrangian decreases the maximum baryon number at which solutions can be found and for any given baryon number the average width, and therefore radius of the star, is decreased. The qualitative features of these solutions, however, are found to be similar to the zero pion mass case.

The solutions found justify allowing the widths and baryon numbers of the shells to vary and show the expected change in baryon density over the radius of the star, with a high density center decreasing rapidly at first and then at a slower rate as the radius increases. This is a more realistic model of a neutron star as the density should increase as the center of the star is reached.

ACKNOWLEDGMENTS

B. P. was supported by an STFC rolling Grant No. ST/G000433/1, and S. N. by an EPSRC studentship.

-
- [1] T. H. R. Skyrme, *Proc. R. Soc. A* **260**, 127 (1961).
 - [2] T. H. R. Skyrme, *Nucl. Phys.* **31** 556(1962).
 - [3] E. Witten, *Nucl. Phys.* **B223**, 422 (1983).
 - [4] P. Bizon and T. Chmaj, *Phys. Lett. B* **297**, 55 (1992).
 - [5] N. K. Glendenning, T. Kodama, and F. R. Klinkhamer, *Phys. Rev. D* **38**, 3226 (1988).
 - [6] M. S. Volkov and D. V. Gal'tsov, *Phys. Rep.* **319**, 1 (1999).
 - [7] H. Luckoek and I. Moss, *Phys. Lett. B* **176**, 341 (1986).
 - [8] S. Droz, M. Heusler, and N. Straumann, *Phys. Lett. B* **268**, 371 (1991).
 - [9] B. M. A. G. Piette and G. I. Probert, *Phys. Rev. D* **75**, 125023 (2007).
 - [10] R. A. Battye and P. M. Sutcliffe, *Phys. Lett. B* **391**, 150 (1997).
 - [11] C. Houghton, N. Manton, and P. Sutcliffe, *Nucl. Phys.* **B510**, 507 (1998).
 - [12] Robert M. Wald, *General Relativity* (University Of Chicago Press, Chicago, 1984).
 - [13] N. S. Manton and B. M. A. G. Piette, *Proceedings of the European Congress of Mathematics, Barcelona 2000*, Progress in Mathematics Vol. 201 edited by C. Casacuberta *et al.* (Birkhauser, Basel, 2001), pp. 469–479.
 - [14] R. A. Battye and P. M. Sutcliffe, *Rev. Math. Phys.* **14**, 29 (2002) <http://www.worldscinet.com/rmp/14/1401/S0129055X02001065.html>.
 - [15] V. B. Kopeliovich, *Pis'ma Zh. Eksp. Teor. Fiz.* **73**, 667 (2001), [*JETP Lett.* **73**, 587 (2001)].
 - [16] V. B. Kopeliovich, *J. Phys. G* **28**, 103 (2002).